



# Beach impacts of shore-parallel breakwaters backing offshore submerged ridges, Western Mediterranean Coast of Egypt

Moheb M. Iskander<sup>a</sup>, Omran E. Frihy<sup>a,\*</sup>, Ahmed E. El Ansary<sup>b</sup>,  
Mohamed M. Abd El Mooty<sup>b</sup>, Hossam M. Nagy<sup>b</sup>

<sup>a</sup>Coastal Research Institute, 15 El Pharaana Street, El Shallalat 21514, Alexandria, Egypt

<sup>b</sup>Faculty of Engineering, Alexandria University, Egypt

Received 25 July 2005; received in revised form 3 November 2006; accepted 18 November 2006

## Abstract

Seven breakwaters were constructed behind offshore submerged ridges to create a safe area for swimming and recreational activities west of Alexandria on the Mediterranean coast of Egypt. Morphodynamic evaluation was based on the modified Perlin and Dean numerical model (ImSedTran-2D) combined with successive shoreline and beach profile surveys conducted periodically between April 2001 and May 2005. Results reveal insignificant morphologic changes behind the detached breakwaters with slight coastline changes at the down and up-drift beaches of the examined breakwaters ( $\pm 10$  m). These changes are associated with salient accretion (20–70 m) in the low-energy leeside of such structures. Concurrent with this sand accretion is the accumulation of a large amount of benthic algae (Sargassum) in the coastal water of the shadow area of these structures, which in turn have adverse effects on swimmers. Practical measures proposed in this study have successfully helped in mitigating such accumulation of algae in the recreation leeside of the breakwaters. The accumulation of Sargassum, together with the virtual insignificant changes in the up-drift and down-drifts of these structures, is a direct response to both coastal processes and the submerged carbonate ridges. Coastal processes encompass reversal of the directions of long-shore sand transport versus shoreline orientation, the small littoral drift rate and sand deficiency of the littoral zone. The beach response to the breakwaters together with the submerged ridges has also been confirmed by applying the ImSedTran-2D model. Results indicate that submerged ridges play a principal role in the evolution of beach morphology along the west coast of Alexandria. Although the study area is exposed to more than 70% wave exposures, the morphodynamic behavior of the beaches indicates that the submerged ridges act in a similar way as an additional natural barrier together with the artificial detached structures. © 2006 Elsevier Ltd. All rights reserved.

**Keywords:** Mediterranean Sea; Detached breakwaters; Submerged ridges; Beach management; Beach morphodynamics

## 1. Introduction

The study area of El Agami is located west of Alexandria on the Mediterranean coast of Egypt and is considered as a principal public resort beach in this region. The 14-km-long coastline of El Agami is oriented SW–NE and is bordered by Abu Talat beach to the west and Agami headland to the east (Fig. 1C and B). To the west, the western Nobaria drain outlet with its pair of jetties limits

Abu Talat beach. The coastline is almost straight and composed of wide beaches covered by white carbonate oolitic sand (Hilmy, 1951). The white sand covers the sub-aerial beach and the near-shore area reflects the water clarity and the unique turquoise color that characterizes this region. These conditions offer esthetic amenities that attract residential construction. As a consequence, rapid and extensive recreation developments in the region have been increasingly undertaken over the last 20 years. However, the main problem facing the beaches of this stretch is their unsuitability for swimming since they are classified between reflective and moderately dissipative beaches and are associated with hazardous rip currents (Nafaa and Frihy, 1993).

\*Corresponding author. Tel.: +203 5276126, mobile: +203 0103078141; fax: +203 4844614.

E-mail address: Frihyomr@link.net (O.E. Frihy).

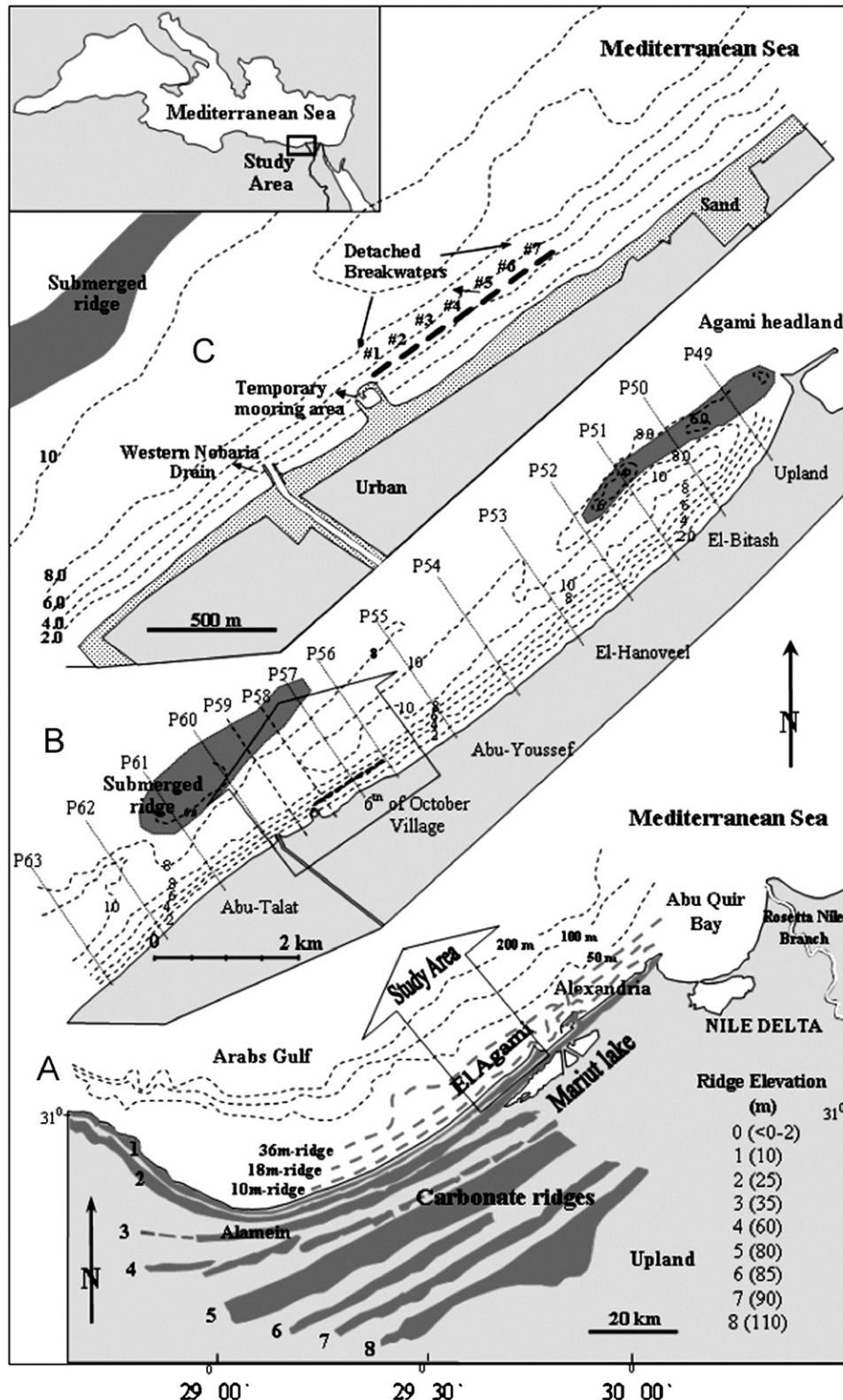


Fig. 1. (A) General map of the Arabs Gulf at the western Mediterranean coast of Egypt showing location of the shore-parallel limestone ridges partially extended across the study area (modified after Butzer, 1960; Misdorp and Sestini, 1975). (B) Location map of El Agami coast and the 15 profiles lines surveyed in this study. (C) Map showing the detached breakwaters constructed on the 6th of October beach west of Alexandria.

These circumstances have encouraged developers to build engineered structured measures in an effect to create sheltered recreational beaches without taking into con-

sideration their harmful impacts on the beach environment (Frihy, 2001). These sheltered beaches are of considerable recreational importance to thousands of people who come

from all over Egypt to use the west coast of Alexandria during summer holidays.

Although the coastline of this area is an open-sea environment, it has experienced long-term dynamic equilibrium through history due to its morphologic nature. The most prominent geomorphologic features are the existence of a series of unconsolidated carbonate ridges which are native to this area, Fig. 1A, the Arabs Gulf in particular (Fourtau, 1893; Shukri et al., 1956; Said et al., 1956; Butzer, 1960; Lindell et al., 1991). The ridges run parallel to the coast in the backshore and in upland areas from Alexandria to Sallum on the Egyptian/Libyan border. They progressively increase in elevation from ~10 m along the coast to ~100 m some 40 km inland (Shukri et al., 1956). Other related ridges extend underwater down to a maximum depth of 20 m across the inner continental shelf of the Arabs Gulf between Alamien and Alexandria as reported by Lindell et al. (1991). The maximum crest height of these ridges is 6–11 m above the seabed and they are generally found in certain water areas of depths ranging between 10 and 15 m. The origin of the inland ridges ranges from marine, such as offshore bars and beach deposits, to eolian (Fourtau, 1893; Shukri et al., 1956; Said et al., 1956; Butzer, 1960). The inland ridges and submerged bedrock are the primary sources of formation of beaches and seabed sediments between Alexandria and Sallum (Hilmy, 1951; Misdorp and Sestini, 1975). The tidal regime along the coast is microtidal semi-diurnal with a mean range of approximately 0.40 m (Debes, 2002).

## 2. Background

The present study is centered on the coastline backing the detached breakwaters along the “6th of October”

beach which were built between 1998 and 2003 west of Alexandria (Fig. 1C and B). The primary function of these breakwaters was not to protect the beach but to provide a safe and secure area for swimming activities. To achieve such a need, seven detached emerged breakwaters made of dolos units were constructed in a water depth between 4 and 5 m and fronting a shoreline of about 1 km long. Each individual breakwater is 100 m in length parallel to the beach, 200 m away from the shore and is spaced at 50 m intervals. A crest level of +1.0 m referenced to MSL was adopted to force the wave energy of the storms. A small temporary harbor was built west of these breakwaters to facilitate construction activities of the breakwaters (Figs. 1C and B and Fig. 2).

It has been observed that sand accretion beyond the detached breakwaters is also associated with accumulation of huge amounts of benthic algae (Sargassum) that impose harmful constraints to swimmers using the protected leeward side of the breakwaters in summer holidays (Fig. 2). Problematic accumulations of algae (Sargassum) have imposed adverse impacts on swimmers using the protected leeward side of the constructed breakwaters.

The purpose of this study is to evaluate changes in the morphology and coastal processes of the littoral zone of El Agami in response of the shore-parallel detached breakwaters and to discuss several factors that have contributed to these changes including the submerged ridges. The analysis presented is based primarily on field measurements (shoreline position, beach profiles, wave pattern, seabed grain sizes and bottom slopes) and supplemented by applying the modified Perlin and Dean numerical model (ImSedTran-2D). Another major objective is to propose an appropriate measure to mitigate the undesirable accumulation of Sargassum in the recreation area, i.e., leeward side of the constructed detached breakwaters.

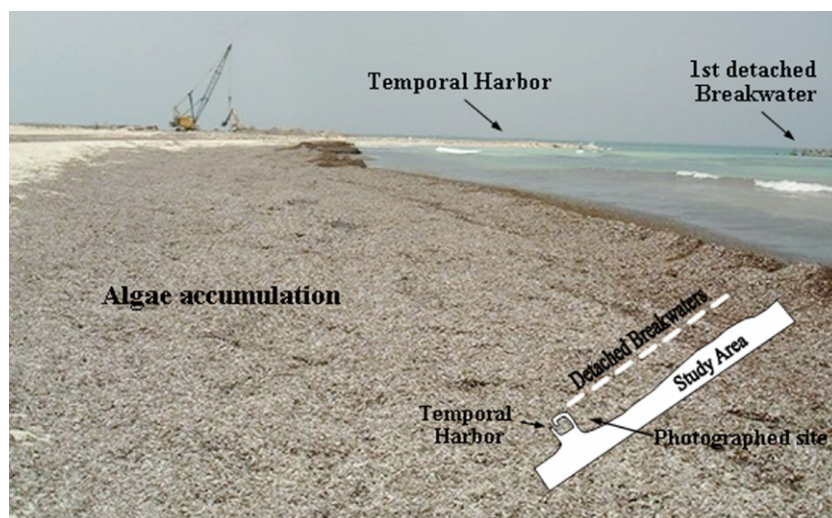


Fig. 2. Photograph (May 2004) showing the detached breakwaters along El Agami beach and accumulation of Algae (Sargassum). Note the temporal harbor and the first detached breakwater (back).



### 3. Methodology

#### 3.1. Field survey

A total of 15 beach-nearshore profiles were surveyed to a depth of 12 m, corresponding to ~1.5 km offshore. These surveys spanned the 14-km length of the study area and were conducted three times over a period of 1 year; from October 2002 to October 2003 (Fig. 1B). The profiles extend from a baseline fixed along the study area with an orientation profile approximately perpendicular to the coastline (Fig. 1B). The distance between profiles ranged between 500 and 1000 m. Seaward of each profile, soundings were taken every 10 m from the baseline up to a depth of about –1.0 m below MWL and then soundings were taken every 3 m up to the 12 m contour depth.

In association with these profile surveys, the initial shoreline position was measured in April 2001 following construction of the first three breakwaters. The profile surveys were carried out during fair-weather using a rubber boat equipped with a DGPS (GBX-Pro) and echo sounder to determine the seasonal variability in shoreline and seabed morphology. The survey elevations, depth and land, are referenced to the Egyptian Survey Authority datum (mean sea level).

During the survey of October 2003, a total of 49 bottom samples were collected at water depths of 2, 4, 6, 8 and 10 m along the profile lines together with two beach samples taken at the swash zone (see Fig. 1B for the profile location). Grain-size analysis was completed in the laboratory by dry sieving using standard ro-tap sieving at  $1\phi$  sieve intervals. The  $\phi$ -scale notation of Krumbein (1963) was used as a size scale. The mean grain size (Mz) for each sample was calculated using the formula of Folk and Ward (1957). The resulting values of Mz in  $\phi$  units were converted into millimeters according to the  $\phi$ -mm transformation: (mm) =  $1/2^\phi$ .

Wave climate (wave height, period and incident wave angle) was analyzed based on available records measured at Damietta Harbor located 220 km east of Alexandria. Although wave characteristics at both localities are much similar waves starting at Abu Quir took about 8 h to reach Ras El-Bar (Fanos et al., 1995). A pressure wave gauge (Inter Ocean System S4DW) was installed at about 12 m deep in the water. The wave gauge recorded the directional wave and current spectrum for 20 min every 4 h. Wave data were compiled for a whole year period from November 2002 to October 2003.

#### 3.2. Model description

The numerical simulation of the coastal processes and sediment transport in the study area was conducted by using the ImSedTran-2D model of Perlin and Dean (1983) with the following modification:

1. The solution was modified to simulate the actual bed contour instead of the ideal bed contour represented by the equilibrium beach profile equation ( $h = AY^{2/3}$ ).

2. The wave diffraction calculation based on the Kraus (1984) solution was added to simulate the bed morphology in the vicinity of the coastal structures. However, the governing equations used to determine the wave direction and wave height distribution for refraction calculations are summarized as follows:

$$\frac{\partial}{\partial x} K \cos \theta - \frac{\partial}{\partial y} K \sin \theta = 0, \quad (1)$$

$$\frac{\partial}{\partial x} \left( \frac{\rho g H^2}{8} C_G \sin \theta \right) + \frac{\partial}{\partial y} \left( \frac{\rho g H^2}{8} C_G \cos \theta \right) = 0, \quad (2)$$

where  $x$  and  $y$  axes are in the long-shore and in the offshore directions, respectively,  $K$  is the wave number,  $\theta$  the wave angle,  $\rho$  the mass density of water,  $g$  the gravitational acceleration,  $H$  the wave height, and  $C_G$  the group velocity.

The wave height at the location in question is simply the product of the specified partially refracted incident wave height and diffraction coefficient. The angle of the wave crest is computed assuming a circular wave front along any radial; this angle is then refracted using Snell's law. Throughout the refraction and diffraction schemes, the local wave heights were limited by the value 0.78 of water depth.

Calculations of the wave distributions are based on shoaling processing, refraction, diffraction, and depth-limited breaking. It is also designed to take the actual wave data measurements at any point offshore of the breaking point.

Then the continuity equation is used to simulate the sediment transport and bathymetry changes:

$$\frac{\partial y}{\partial t} + \frac{\partial q_x}{\partial x} + \frac{\partial q_y}{\partial y} = 0, \quad (3)$$

where  $q_x$  and  $q_y$  represent the long-shore and cross-shore sediment transport, respectively.

$Q_x$  is given by (Perlin and Dean, 1983)

$$Q_{x_{ij}} = \left\{ \left[ \exp - \left( \frac{(y_{i,j-1}) + H_{b_i}}{1.25 y_{b_i}} \right)^3 - \exp - \left( \frac{(y_{i,j}) + H_{b_i}}{1.25 y_{b_i}} \right)^3 \right] \times \frac{K_l}{(\rho_s - \rho)g(1-p)} E_{b_i} C_{g_{b_i}} \sin(2\alpha'_{i,j} - 2\alpha_{c_{i,j}}) \right\}. \quad (4)$$

$Q_{x_{ij}}$  represents the long-shore sediment transport between depths  $d_{i,j}$  and  $d_{(i,j-1)}$ ,  $\alpha'_{i,j}$  the averaged wave angle at the location of  $Q_{x_{ij}}$ , and  $\alpha_{c_{i,j}}$  the local contour orientation angle,  $H_{b_i}$  the breaking wave height at “ $i$ ” grid-line along the  $x$  direction, and  $p$  the prosiety.

$Q_y$  is given by (Bakker, 1968)

$$Q_{y_{ij}} = \Delta x K_{c_{ij}} [y_{i,j-1} - y_{i,j} + W_{EQ(i,j)}]. \quad (5)$$

$Q_{y_{ij}}$  represents the cross-shore sediment transport,  $K_c$  is an activity factor and  $W_{EQ(i,j)}$  is the positive equilibrium profile distance between  $y_{i,j}$  and  $y_{(i,j-1)}$ .

To solve the finite-difference form of the continuity equation boundary values (left side, right side, onshore, and offshore boundaries of the study area) are required. The “ $y$ ” values along the left- and right-side boundary are assumed to be fixed at their initial locations. This means that the sediment transport quantity along these boundaries is zero. The onshore boundary is treated by assuming that the berm and beach face move in conjunction with the shoreline position. The offshore boundary is treated by keeping the contour beyond the last simulated one fixed until the bed slope transcends the angle of repose then resetting it to a position such that the slope equals the angle of repose. For more details on the model see Perlin and Dean (1983), and for the modification see Iskander (2005).

#### 4. Profile variability and sediment grain size

Beach profiles are used to understand and quantify the variations in seabed levels and shoreline orientation, which are undergoing continuous change in response to the marine processes such as waves and currents. Results of the profile analysis reveal cross-shore marked variability in the irregularity of the seabed morphology, slope and grain size distribution. The most distinctive characteristic of the littoral cell is its marked bathymetry due to the existence of bedrock limestone features covered partially by carbonate sand. Visual examination of the constructed bathymetry and profile configurations revealed shore-parallel submerged ridges (Fig. 3a and b). The beach-face and surf-zone down to 10 m depth are mostly covered by loose carbonate sand, while the offshore bedrock is partially exposed. These bedrock outcrops form the most pronounced morphological feature in this region. Parts of these outcrops extend above the mean water level to form shore-parallel islets fronting the coastline. Profile #P58 has been taken as an example to display the rough irregularities in the seabed of this area (Fig. 3a). The ridge crest is about 1250 m seaward and 500 m wide at its base. The crest is elevated 6–11 m from the seabed (Fig. 3a). This seabed configuration is more or less typical for the classical coastal topography along the Alexandria littoral cell (Frihy et al., 2004).

Unlike the Nile delta, microscopic examination of beach and seabed samples indicates that they are mainly comprised of carbonate grains (95%), quartz grains (4%) and shell fragments (1%). Heavy minerals rarely occurred in beach and seabed samples. In general, the mean grain size of the beach and bottom sediment increases in a seaward direction (Fig. 3b). The fine-grained sediments (0.11–0.51 mm) mostly cover the beach and nearshore zone whereas the coarse-grained sediments (0.51–0.74 mm) occur mostly further offshore beyond the 8.0–10.0 m depth contour where the submerged ridges are located. The only exception is that sediment near the rocky ridges, especially along profile 58, which is relatively coarse with a maximum peak of 0.7 mm, exists at 6.0 m depth contour (Fig. 3b). A similar seaward coarsening trend is also observed along

the littoral cell of Alexandria due to the existence of relict late Pleistocene to mid-Holocene coarse-grained sand offshore beyond the 8–10 m water depth (Frihy et al., 2004).

The cross-shore seabed slope of the study area generally decreases from 0.20 in the beach-face to 0.02 in the surf-zone. In the along-shore direction, the beach-face between +1.0 and −1.0 m is relatively steeper averaging 0.10 (Fig. 3c). Generally, the beach-face slope systematically decreases eastwards from ~0.20 near Abu Talat to ~0.04 near El Agami Headland. A relatively gentle seabed slope of 0.04 is observed in the lee-side of the detached breakwaters due to the effect of the salient accretionary formation. The swash zone is characterized by having coarser sediment ( $M_z = 0.5–0.7$  mm) on a steeper slope surface (0.1) than the surf-zone which is relatively finer ( $M_z = 0.2$  mm) and less steep (0.02).

#### 5. Beach morphodynamics

By analyzing 1 year of actual wave measurement data, the average significant wave height and period are 1.04 m and 6.2 s, respectively with a maximum wave height of 4.45 m blown from NW in winter. The N, NNW and NW waves are important in inducing morphological changes because of their long duration particularly in winter. The remaining NNE and NE components occasionally occur during April and May.

It has been established that when waves approach the coast at an angle, they cause sediment to be transported along the shore i.e., long-shore sediment transport. The direction and magnitude of long-shore current and littoral drift depend on the effective angle of incident waves and average shoreline orientation. The relationship between wave climate and the present shoreline orientation (57° from the north) provides effective oblique wave exposures (Fig. 4a). Accordingly, two main wave exposures are responsible for generating opposing SW and NE long-shore sediment transport (see the two arcs in Fig. 4a). In general, the predominant wave components propagating from NW, WNW, and W sectors, 85% of the time, are responsible for the generation of long-shore currents towards the northeast, representing up to 70% of the total wave distribution. Approximately 10% of the time waves approach from NNW, N, NNE, and NE, on the other hand, and generate a reverse long-shore current towards the southwest, particularly during March and April, in total contributing ~19% of the wave distribution (Fig. 4a). The remaining component (11%) represents calm conditions generally with S and SE waves, i.e., from the inland direction, spanning ~5% of the time. Evidence for this small net littoral drift has come from field observations of sand accumulation patterns adjacent to the jetties constructed to protect west Nobarra Drain and on both sides of the small temporal harbor built in the study area.

The model is applied to calculate the wave distributions across the study area using the bathymetry map of October

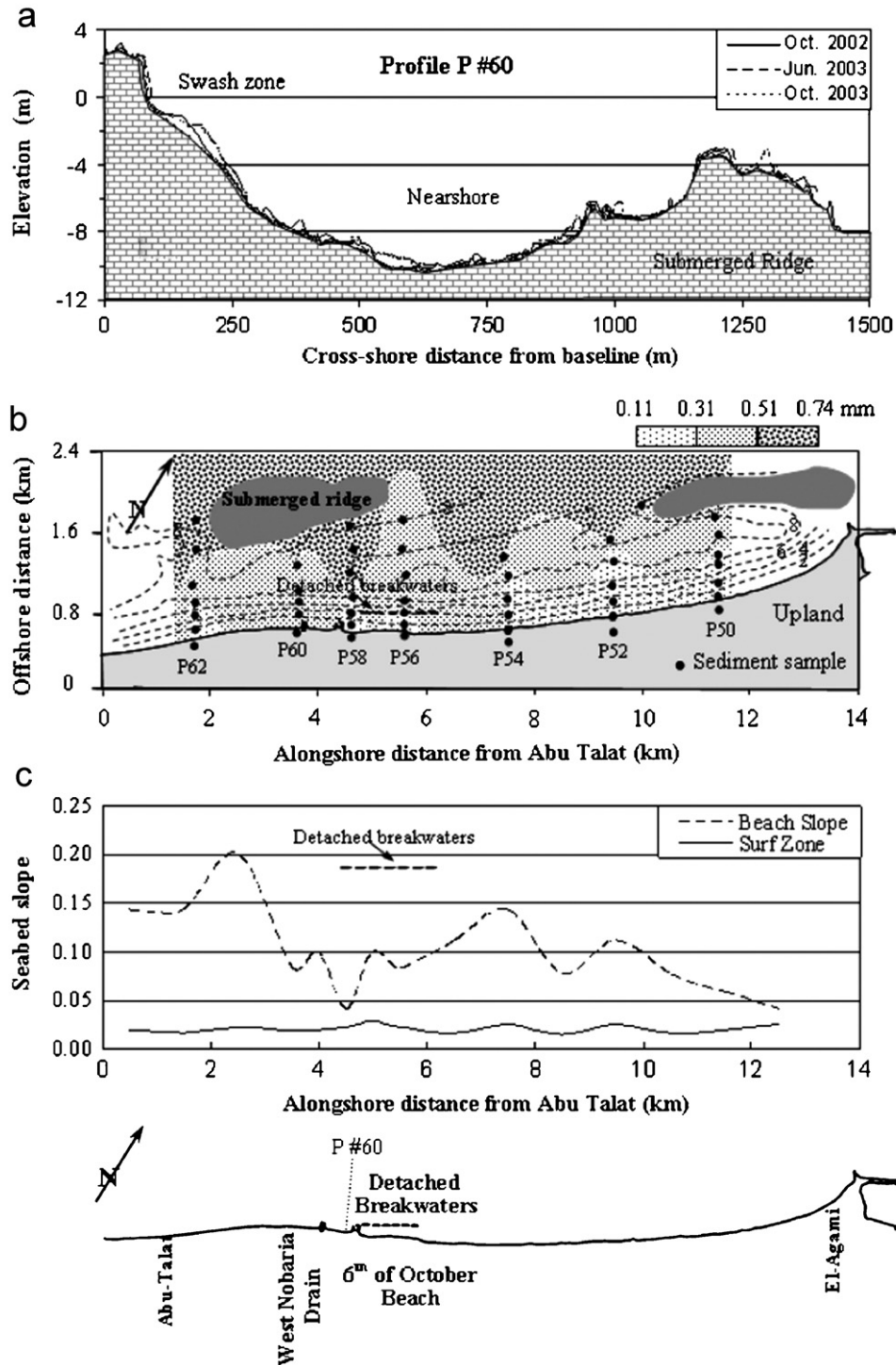


Fig. 3. (a) Pronounced seabed morphologic features along the study area as depicted from profile P #60. The surface of the submerged ridge with its high relief accelerates wave breaking thus reducing wave energy reaching the breakwaters. (b) Spatial distribution of mean grain size (c) Beach slope and surf zone of the study area.

2002 for both the significant and maximum wave heights. Because of space limitations, the distribution of significant wave height and direction, resulting from  $H_s = 1.04$  m,  $T_s = 6.2$  s and direction =  $290^\circ$  from the north, is shown in Fig. 4b. Wave distribution in the sheltered zone of the breakwater behaves in a refracted and diffracted pattern.

Wave heights notably decrease beyond the western breakwaters due to the double sheltering effect of these breakwaters and the temporal harbor.

To quantify the changes in the shoreline positions and bottom contours observed in the study area, the initial surveys of April 2001 and May 2005 are graphically plotted

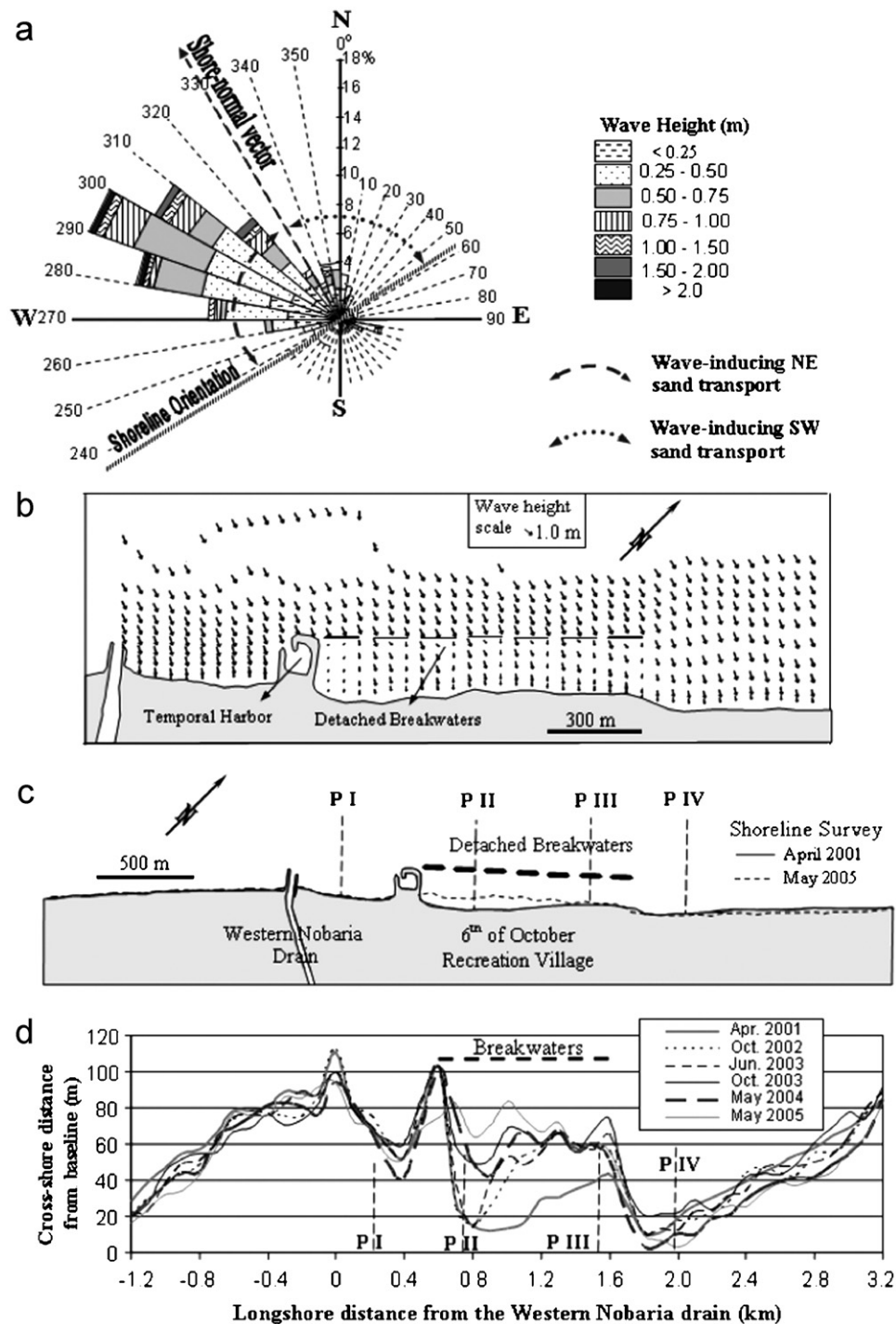


Fig. 4. (a) Wave climate (wave rose and average orientation of the coastline) and the two main wave exposures inducing northeasterly and southwesterly sediment transport pathways. (b) Modeled spatial wave distribution along the study area. (c) Along-shore changes in shoreline positions from baseline (m). (d) Long-shore shoreline changes and position of the four profiles (I–IV) used in the model calibration and verification.

in Fig. 4c. The along-shore changes in all survey periods are examined in more detail using the bivariate plot in Fig. 4d. The variations in shoreline positions on both sides of the detached breakwaters along both the up-coast and down-coast are relatively small, fluctuating between  $\pm 10$  m. During the period from April 2001 to May 2005, the average retreat of the shoreline up-coast of the breakwaters reached 8.0 m while it reached 10 m in the

down-coast. These two coastal stretches extend about 1.5 km on both sides of the breakwaters. It is likely that this erosion/accretion fluctuation is changeable, rather than continuous, due to the seasonal variation in wave climate and reversibility in the direction of long-shore sand transport, to the NE and to the SW (Fig. 4a). In contrast, the shoreline of June 2003 beyond the detached breakwaters advanced seaward by  $\sim 35$  m since the initial 2001 survey



(Fig. 4d). This accretion occurred following construction of the first three breakwaters in June 2003 and gradually increased afterwards. In the same locality, the shoreline of May 2005 accreted seaward ranging between 20 and 70 m, with an average value of 40 m, spanning 4 years from the initial survey of April 2001.

Comparison between the survey conducted immediately before May 2004 and after removal of the temporal harbor in May 2005 indicates that the beach width diminished eastward and the shoreline tends to be parallel to the breakwaters (Fig. 4d). The accretion/erosion patterns during this period ranged between  $\pm 25$  m with a general trend of sand accumulation at an average of 6.0 m. This degree of sand accretion beyond the detached breakwaters is also associated with accumulation of huge amounts of Sargassum, which disrupts swimming activities during the sheltered areas in summer holidays (Fig. 2). Considerable efforts were made to mechanically remove this algae but accumulation has reoccurred. An accumulation of Sargassum has been also detected in this region using remote sensing in depressions confined between submerged ridges in the Arabs Gulf (Lindell et al., 1991). This problem was totally solved following dismantling of the temporary harbor in May 2005.

In general, the observed morphology of shoreline and seabed contours is unlike that previously established in common responses to detached breakwaters. Commonly, erosion occurs in the gaps, tombolos or salients in the wave shadows of each breakwater and significant changes might be expected on both sides of the breakwater system. Within 5 years (1998–2003), during all stages of the breakwaters construction, the configuration pattern of the shoreline and bottom contours seemed to be more or less linear with no pronounced undulating features that may exist behind the breakwaters (Fig. 1C and B). In comparison, the observed beach morphology along the study area does not resemble the sedimentation pattern observed at Marabella breakwaters, about 62 km west of El Agami, where no ridges have been observed. Unlike the El Agami breakwaters, the rapidly formed tombolos in the shadow zone of those breakwaters have blocked the sediment flow to the east, thus contributing to beach erosion at the downdrift side of these structures (Frihy, 2001).

The morphologic performance in the vicinity of the breakwaters gives an indication of the influence of the submerged existing seaward ridges of such structures. A remnant submerged ridge, possibly the inner one (coastward), was detected during all sounding surveys (Fig. 1B). The sheltering effect of such ridges provides a natural protection system for this coastal stretch. Incoming waves break and their energy dissipates on the ridge crest, thereby sheltering the littoral zone hosting the breakwaters. From field observation, we noticed that the breakwater provides much less wave energy at the beach-face when the ridge is present. Acting together with this hydrodynamic response is the very limited littoral drift. The net littoral drift potential in the area appears to be relatively moderate at an

approximate rate of  $0.42 \times 10^6 \text{ m}^3/\text{year}$  (El-Fishawi, 1994). Another factor is that the littoral cell faces a substantial deficit in sand supply due to its self-contained source. Beach and seabed sediment of the surf-zone mainly originate from eroded carbonate ridges along the coast and their contiguous bedrock.

## 6. Modeling

The modified Perlin and Dean numerical model (ImSedTran-2D) was used to examine the variability of the beach profiles under two conditions: firstly, dealing with the existing condition in which both the detached breakwaters and submerged ridges exist, and secondly, applying the model with the assumption that the temporal harbor built to serve breakwater construction works had been removed. Prior to dealing with these two conditions, the model was initially calibrated.

### 6.1. Model calibration

The constructed contour maps obtained from the surveyed profiles along with the wave data and mean grain size of the seabed sediments were used to calibrate the ImSedTran-2D model to be applied in the vicinity of the detached breakwaters. The field data used spanned the 12 months between October 2002 and October 2003. Starting with the initial survey of October 2002, a series of simulations/runs were carried out in order to reproduce the true seabed contours of October 2003 (Fig. 5a). In each run, the calibration parameters of the model including the activity factor, the long-shore equation factor and the breaking wave energy parameter were carefully adjusted to simulate bottom contours comparable with the original field data surveyed in October 2003. The activity factor adjusts the cross-shore sediment transport. The long-shore transport equation factor controls the long-shore transport. The breaking wave energy parameter represents the effect of the breaking wave energy, which occurs primarily near the water surface, on the sediment transport near the bed. This calibration procedure suggested values of these parameters to be 0.00001, 0.0035, 1.0, respectively.

A comparison between the measured and calculated bathymetric survey of October 2003 is depicted along four selected cross-shore profiles shown in Fig. 5. Profiles #I and #IV are positioned, respectively, in the up-drift and lee sides of the breakwaters, whereas Profiles #II and #III are located within the breakwater zone (Fig. 4c). These profiles served as the basis to quantify bottom changes as a function of existing conditions i.e., the presence of both the detached breakwaters and ridges. The seabed variability in these profiles shows a good agreement between the measured and calculated seabed morphology. The relative similarity of seabed configuration in each profile confirms the high compatibility of both the simulated seabed and the field survey, i.e.,



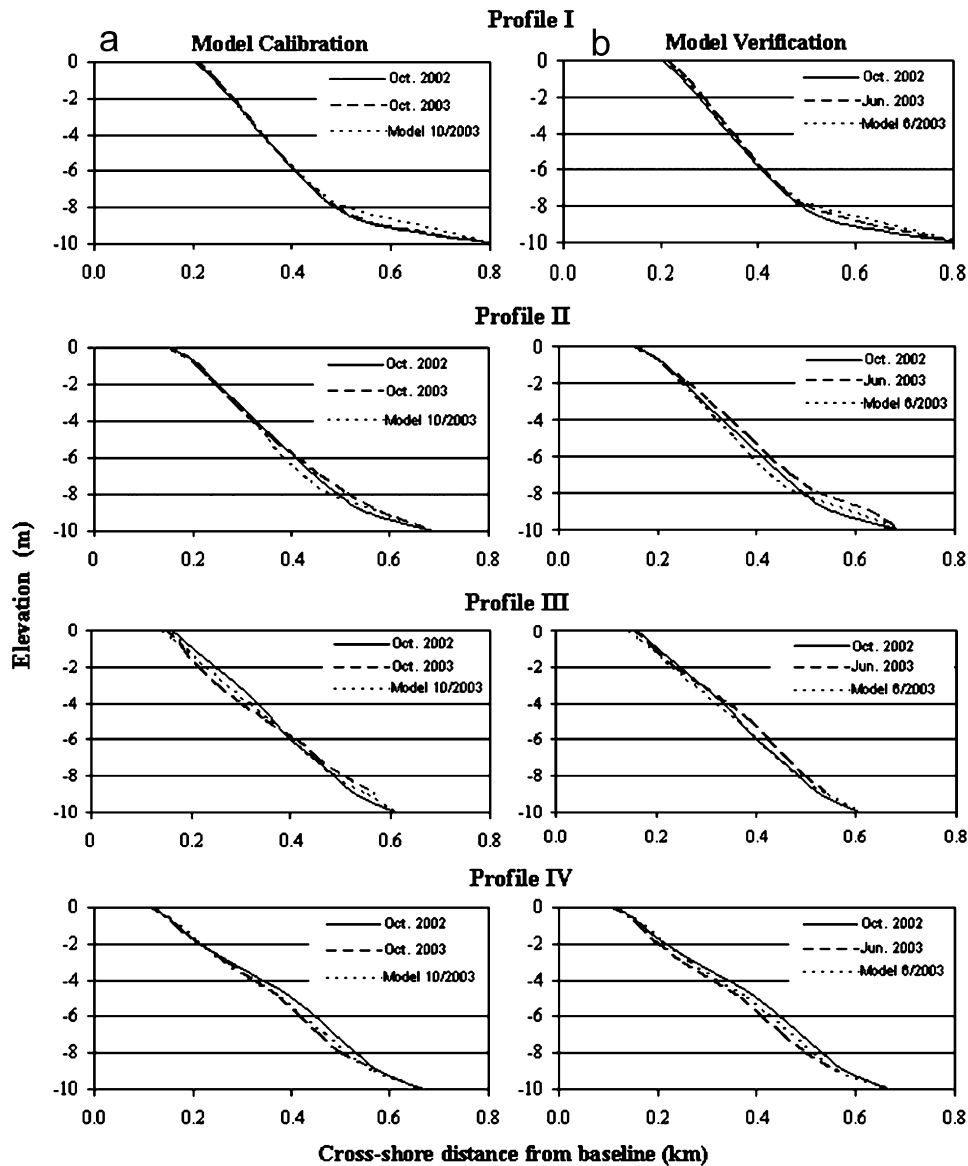


Fig. 5. Model calibration (a) and model verification (b), showing comparison between predicted seabed topography and field measurements across four selected profiles. Profile positions are shown in Fig. 4c.

the model predictions correspond well with the field observations.

### 6.2. Model verification

The next step was to verify the model. The bathymetric survey of June 2003 together with the available wave data measured between October 2002 and June 2003 was used in the verification processes using the justified calibration parameters. Results of such verification are depicted as seabed configuration along the same profile lines used above in the processes of calibration (Fig. 5b). The small difference between the field data and the model results is perhaps related to inaccurate simulation of the submerged ridges in the model. The changes in the spatial variability of the seabed along the examined profiles were a bit different due to dissipation of incident waves

crossing the ridges and the breakwaters. Insignificant seabed accretion appeared just west of the detached breakwaters whereas relative erosion occurred to the lee side east of the breakwaters. This slight erosion/accretion pattern reflects the limited effect of the breakwaters due to the existing ridges. In contrast, marked accretion exists in the shadow area of the breakwaters associated with local erosion near the deeper part of the surf-zone due to the effect of winter storms. Of importance is that the resulting bathymetry shows relatively straight and simple seabed contours.

### 6.3. Model application

The calibrated model was also used to answer the following question: What would happen if the small temporary harbor built west of the structure were to be

dismantled? The results obtained, as anticipated, following application of the model indicated that the sedimentation will be enhanced in a short time without major disturbance to beach morphology. A landward shift between depth contours varying between 1.0 and 2.0 m would occur. On the other hand, harbor dismantling would gently increase water flow between the shoreline and breakwaters and thus would virtually eliminate accumulation of dead algae in the swimming water.

#### 6.4. The empirical equations

Offshore breakwaters have been used successfully to control shoreline evolution when the dimensions of such structures are correctly defined. These dimensions include the breakwater crest height ( $H$ ), effect of the offshore distance of the breakwater ( $X$ ), the length ( $B$ ) and the breakwater gap ( $G$ ). In this study, we applied the empirical design equations for the detached breakwaters developed by Herlich (1991), Hallermeier (1983), Seiji et al. (1987), Hsu and Silvester (1990) in an attempt to test the validity of these equations. Results indicate that the dimensions used in designing the El Agami breakwaters are comparable with cases producing minimum morphologic changes. In our case, morphologic responses appeared in the form of a salient with a maximum length of 40 m. In addition, associated beach erosion facing breakwater gaps seems to be minimal with a nearly straight shoreline and bottom contours.

#### 7. Summary and conclusions

This study dealt with the effect of submerged ridges in controlling profile evolution in the vicinity of detached breakwaters built to stabilize the recreation beach at El Agami on the west coast of Alexandria. Of particular importance is the role of the carbonate ridges in dissipating incoming waves, which influence the hydrodynamic field that in turn affects sediment transport processes in the vicinity of such structures.

Field observations spanning 4 years of shoreline position and beach profile data indicated that there has been no significant effect of the breakwaters on the adjacent shoreline and seabed contours. In the along-shore direction, both the down- and upcoast of the breakwaters show small changes ( $\pm 10$  m), with a considerable salient accretion (20–70 m) in the lee side of these structures. Another change observed was an accumulation of Sargassum in the swimming area between the shore and the detached breakwaters. The considerably smaller spatial morphologic variability documented in this coastal stretch doesn't conform to the "classic" forms described elsewhere behind breakwaters due to the effect of a combination of several factors. Of particular importance is the existence of the offshore submerged ridges which effectively dissipate the energy of the deep water incident waves before reaching the breakwaters and thus act as additional natural shore-

parallel barriers and perform the same functions as those described for offshore breakwaters. Other factors, are the effect of shoreline orientation on the sediment transport direction due to the action of coastal processes, and the smaller littoral drift rate and sediment deficiency within the surf zone.

Although the examined beach was classified as reflective to moderately dissipative, the beach morphology tends to quickly shift to a more fully dissipative stage, effectively breaking the wave energy on the ridge surface before reaching the breakwaters.

Lessons learned from this study are relevant to numerous engineering endeavors such as the assessment of beach stability, design of coastal structures, as well as predictions of the dynamic response of coastal protection structures. Results of this study indicate that raised bedrock systems that allow wave dissipation, can be utilized in artificial protection works. For example, raised bedrock features can be used as a toe or as a foundation base for protective structures such as detached breakwaters or as offshore shelters for beach nourishment projects. Another lesson is that detailed bathymetric surveys over a much wider area of a structure and surrounding seabed are necessary for engineering purposes where knowledge of the submerged morphologic features and coastal processes within the study area is required. Understanding the contribution of these ridges in coastal protection is an important topic for further research.

#### References

- Bakker, W.T., 1968. The dynamics of a coastal with a groin system. In: Proceedings of the 11th Conference on Coastal Engineering. ASCE, New York, pp. 492–517.
- Butzer, K.W., 1960. On the Pleistocene shorelines of Arabs' Gulf, Egypt. *Journal of Geology* (68), 626–637.
- Debes, A.M., 2002. The study of sea level changes and currents at Rosetta and Damietta Outlets and Abu Quir Bay. M.Sc. Thesis, Physical Oceanography Department, Faculty of Science, Alexandria University, 150pp.
- Fanos, A.M., Naffaa, M.G., Fouad, E.E., Omar, W.A., 1995. Seasonally and yearly wave regime and climate off the Mediterranean coast of Egypt. In: Proceedings of the Fourth International Conference on Coastal and Port Engineering in Developing Countries (COPEDEC IV), Rio de Janeiro, Brazil, pp. 2075–2093.
- El-Fishawi, N.M., 1994. Characteristic of Littoral Drift along the Nile Delta Coast I: Alexandria—Burullus. *INQUA, MBSS, Newsletter* (16), 38–44.
- Folk, R.L., Ward, W.C., 1957. Brazos River Bar: a Study in the Significance of Grain Size Parameters. *Journal of Sedimentary Petrology* (27), 3–27.
- Fourtau, R., 1893. La region de Maryut; 'etude Geologique. *Bulletin de l'Institut d'Egypt*, ser. 3, 141pp.
- Frihy, O.E., 2001. The necessity of environmental impact assessment (EIA) in implementing coastal projects: lessons learned from the Egyptian Mediterranean Coast. *Journal of Ocean and Coastal Management* (44), 489–516.
- Frihy, O.E., Iskander, M.M., Badr, A.E., 2004. Effect of shoreline and bedrock irregularities on the morphodynamics of Alexandria Coast Littoral Cell, Egypt. *Geo-Marine Letters* 24 (4), 195–211.
- Hallermeier, R.J., 1983. Sand transport limits in coastal structure design. In: Proceedings of the International Conference on Coastal Structures '83. ASCE, New York, pp. 703–716.

- Herbich, J.B., 1991. Handbook of Coastal and Ocean Engineering. Gulf Published, Houston, TX, 1340pp.
- Hilmy, M.E., 1951. Beach sands of the Mediterranean Coast of Egypt. *Journal of Sedimentary Petrology* 1 (21), 109–120.
- Hsu, J.R., Silvester, R., 1990. Accretion behind single offshore breakwater. *Journal of Waterway, Port, Coastal, and Ocean Engineering*, ASCE (116), 362–380.
- Iskander, M.M., 2005. Simulating some coastal problems in Egypt using numerical modeling. Ph.D. Thesis, Faculty of Engineering, Alexandria University, 170pp.
- Kraus, N.C., 1984. Estimate of breaking wave height behind structures. *Journal of Waterway, Port, Coastal, and Ocean Engineering*, ASCE 110, 276–282.
- Krumbein, W.C., 1963. Application of logarithmic moments to size frequency distributions of sediments. *Journal of Sedimentary Petrology* 6, 35–47.
- Lindell, L.T., Alexandersson, E.T., Norman, J.O., 1991. Satellite mapping of oolitic ridges in Arabs Gulf, Egypt. *Journal of Geocarto International*, Sweden (1), 49–60.
- Misdorp, R., Sestini, G., 1975. The Nile Delta: main features of the Continental Shelf topography. In: *Proceedings of Seminar on Nile Delta Sedimentology*, Alexandria, Egypt, pp. 145–161.
- Nafaa, M.G., Frihy, O.E., 1993. Beach and nearshore features along the dissipative coastline of the Nile Delta, Egypt. *Journal of Coastal Research* 1 (9), 423–433.
- Perlin, M., Dean, R.G., 1983. A numerical model to simulate sediment transport in the vicinity of coastal structures. *Miscellaneous Report No. 83-10*, US Army, Corps of Engineers, CERC, Fort Belvoir, 199pp.
- Said, R., Philip, G., Shukri, N.M., 1956. Post Tyrrhenian climatic fluctuations in Northern Egypt. *Quaternaria* (3), 167–172.
- Seiji, M., Uda, T., Tanaka, S., 1987. Statistical study on the effect and stability of detached breakwaters. *Journal of Coastal Engineering in Japan* (30), 131–141.
- Shukri, N.M., Philip, G., Said, R., 1956. The geology of the Mediterranean Coast between Rosetta and Bardia, Part II, Pleistocene sediments: geomorphology and microfacies. *Bulletin de l'Institut d'Egypt* (37), 395–427.